Velocity circulation statistics in counterflow turbulence

P. Z. Stasiak
School of Mathematics, Statistics and Physics, Newcastle University, Newcastle upon Tyne, NE1 7RU, United Kingdom

G. Krstulovic
Université Côte d'Azur, Observatoire de la Côte d'Azur, CNRS,Laboratoire Lagrangre, Boulevard de l'Observatoire CS 34229 - F 06304 NICE Cedex 4, France

L. Galantucci
Istituto per le Applicazioni del Calcolo "M. Picone" IAC CNR, Via dei Taurini 19, 00185 Roma, Italy
(Dated: February 3, 2026)

Lorem ipsum dolor sit amet, consectetuer adipiscing elit. Etiam lobortis facilisis sem. Nullam nec mi et neque pharetra sollicitudin. Praesent imperdiet mi nec ante. Donec ullamcorper, felis non sodales commodo, lectus velit ultrices augue, a dignissim nibh lectus placerat pede. Vivamus nunc nunc, molestie ut, ultricies vel, semper in, velit. Ut porttitor. Praesent in sapien. Lorem ipsum dolor sit amet, consectetuer adipiscing elit. Duis fringilla tristique neque. Sed interdum libero ut metus. Pellentesque placerat. Nam rutrum augue a leo. Morbi sed elit sit amet ante lobortis sollicitudin. Praesent blandit blandit mauris. Praesent lectus tellus, aliquet aliquam, luctus a, egestas a, turpis. Mauris lacinia lorem sit amet ipsum. Nunc quis urna dictum turpis accumsan semper.

INTRODUCTION

Lorem ipsum dolor sit amet, consectetuer adipiscing elit. Etiam lobortis facilisis sem. Nullam nec mi et neque pharetra sollicitudin. Praesent imperdiet mi nec ante. Donec ullamcorper, felis non sodales commodo, lectus velit ultrices augue, a dignissim nibh lectus placerat pede. Vivamus nunc nunc, molestie ut, ultricies vel, semper in, velit. Ut porttitor. Praesent in sapien. Lorem ipsum dolor sit amet, consectetuer adipiscing elit. Duis fringilla tristique neque. Sed interdum libero ut metus. Pellentesque placerat. Nam rutrum augue a leo. Morbi sed elit sit amet ante lobortis sollicitudin. Praesent blandit blandit mauris. Praesent lectus tellus, aliquet aliquam, luctus a, egestas a, turpis. Mauris lacinia lorem sit amet ipsum. Nunc quis urna dictum turpis accumsan semper. Lorem ipsum dolor sit amet, consectetuer adipiscing elit. Etiam lobortis facilisis sem. Nullam nec mi et neque pharetra sollicitudin. Praesent imperdiet mi nec ante. Donec ullamcorper, felis non sodales commodo, lectus velit ultrices augue, a dignissim nibh lectus placerat pede. Vivamus nunc nunc, molestie ut, ultricies vel, semper in, velit. Ut porttitor. Praesent in sapien. Lorem ipsum dolor sit amet, consectetuer adipiscing elit. Duis fringilla tristique neque. Sed interdum libero ut metus. Pellentesque placerat. Nam rutrum augue a leo. Morbi sed elit sit amet ante lobortis sollicitudin. Praesent blandit blandit mauris. Praesent lectus tellus, aliquet aliquam, luctus a, egestas a, turpis. Mauris lacinia lorem sit amet ipsum. Nunc quis urna dictum turpis accumsan semper. Lorem ipsum dolor sit amet, consectetuer adipiscing elit. Etiam lobortis facilisis sem. Nullam nec mi et neque pharetra sollicitudin. Praesent imperdiet mi nec ante. Donec ullamcorper, felis non sodales commodo, lectus velit ultrices augue, a dignissim nibh lectus placerat pede. Vivamus nunc nunc, molestie ut, ultricies vel, semper in, velit. Ut porttitor. Praesent in sapien. Lorem ipsum dolor sit amet, consectetuer adipiscing elit. Duis fringilla tristique neque. Sed interdum libero ut metus. Pellentesque placerat. Nam rutrum augue a leo. Morbi sed elit sit amet ante lobortis sollicitudin. Praesent blandit blandit mauris. Praesent lectus tellus, aliquet aliquam, luctus a, egestas a, turpis. Mauris lacinia lorem sit amet ipsum. Nunc quis urna dictum turpis accumsan semper.

METHOD

Superfluid dynamics are modelled by employing the recently developed FOUCAULT model [1]. We follow Schwarz's approach [2], by exploiting the large separation of scales between the ^{4}He vortex core size a_0 and the average inter-vortex spacing ℓ. We parametrize the superfluid vortex lines as 1D space curves $\mathbf{s}(\xi, t)$ with ξ and t the arclength and time respectively. The corresponding equation of motion is

$$\dot{\mathbf{s}}(\xi, t) = \mathbf{v}_{s_\perp} + \beta \mathbf{s}' \times \mathbf{v}_{ns} + \beta' \mathbf{s}' \times [\mathbf{s}' \times \mathbf{v}_{ns}] \quad (1)$$

where $\mathbf{s}' = \partial \mathbf{s}/\partial \xi$ is the unit tangent vector at $\mathbf{s}$, $\mathbf{v}_{ns} = \mathbf{v}_n - \mathbf{v}_s$ where $\mathbf{v}_n$ and $\mathbf{v}_s$ are the normal fluid and superfluid velocities at $\mathbf{s}$, and β, β' are temperature and Reynolds number dependent mutual friction coefficients. The superfluid velocity $\mathbf{v}_s$ is computed via a desingularized Biot-Savart integral, accelerated using the tree algorithm [3] (see Supplementary Materials). We describe the normal fluid in a classical way, using the

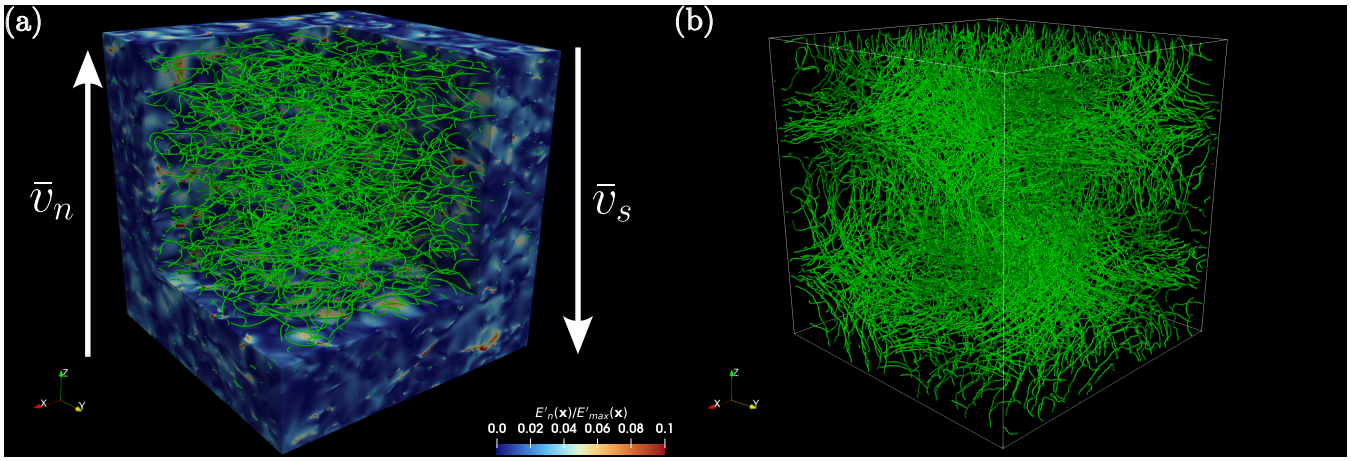

FIG. 1: Visualisation of turbulent vortex tangles. (a) Counterflow-induced turbulence generated at $T = 2.1$ K with a counterflow velocity of $v_{ns} = \bar{v}_n - \bar{v}_s = 0.94$ cm/s. The blue and red surface rendering shows the normalised kinetic energy density of normal fluid fluctuations E'_n/E'_{max} where $E'_n = |\mathbf{v}_n - \bar{\mathbf{v}}_n|^2$. (b) Turbulence generated by an initial Taylor-Green configuration (see Supplementary Materials for details). In both (a) and (b) superfluid vortex lines are represented as green tubes with exaggerated size.

incompressible ($\nabla \cdot \mathbf{v}_n = 0$) Navier-Stokes equation

$$\frac{\partial \mathbf{v}_n}{\partial t} + (\mathbf{v}_n \cdot \nabla)\mathbf{v}_n = -\frac{1}{\rho}\nabla p + \nu_n \nabla^2 \mathbf{v}_n + \frac{\mathbf{F}_{ns}}{\rho_n} \qquad (2)$$

where ρ_n and ρ_s are the normal fluid and superfluid densities, $\rho = \rho_n + \rho_s$, p is the pressure, ν_n is the kinematic viscosity of the normal fluid and $\mathbf{F}_{ns}$ is the mutual friction force per unit volume.

In this study, we prepare two distinct turbulent vortex tangles generated by (a) a $T = 2.1$ K thermal counterflow (CF) with an average inter-vortex distance ℓ_{CF} and (b) a $T = 0$ K evolution of a tangle with a Taylor-Green initial condition (TG) with an average inter-vortex spacing ℓ_{TG}. Both of these tangles are visualized in the left and right panels of Fig. 1 respectively. The velocity circulation statistics of $\mathbf{v}_s$ are obtained by a vorticity coarse-graining process described in the Supplementary materials. Furthermore, the statistics related to the counterflow are decomposed into the normal fluid (NF) and superfluid (SF) components. Each of these components are further decomposed into the perpendicular ($\perp$) and ($\parallel$) components, corresponding to the directions over which statistics are averaged. Perpendicular (parallel) relates to the statistics averaged in the direction where the flux of vorticity through a square loop of size r is perpendicular (parallel) to the counterflow velocity $\mathbf{v}_{ns}$.

RESULTS

Firstly, we begin by considering the simplest observable for velocity circulation statistic - the variance $\langle|\Gamma|^2\rangle$ for different loop sizes r. The circulation variance scalings are shown in Fig. 2, where we have identified two

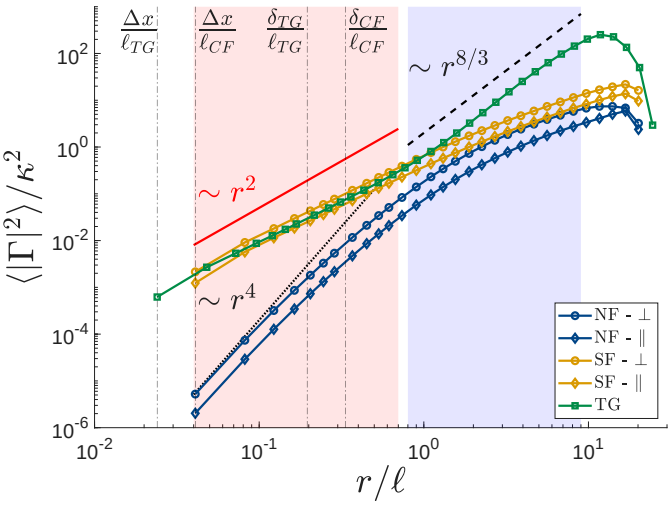

FIG. 2: Circulation variance $\langle|\Gamma|^2\rangle$ around square loops of size r. The blue and yellow curves show the normal fluid and super fluid simulations respectively, which are subdivided into the perpendicular (circles) and parallel (diamonds) components. The green squares show the Taylor-Green simulation.

scaling regimes, a quantum regime $r \ll \ell$ with red shading and a classical regime $r \gtrsim \ell$ with blue shading. Indeed in the quantum regime we find good agreement for the superfluid velocity statistics with the small-scale theory $\langle|\Gamma^2|\rangle \sim r^2$ as discussed in Ref. [4] using the Gross-Pitaevskii (GP) model. We observe that in this regime the scaling not only follows the GP theory, but the quantum region scaling is independent of thermal effects and the nature of the turbulent driving force. Similarily, the normal fluid also exhibits the well known viscous scal-

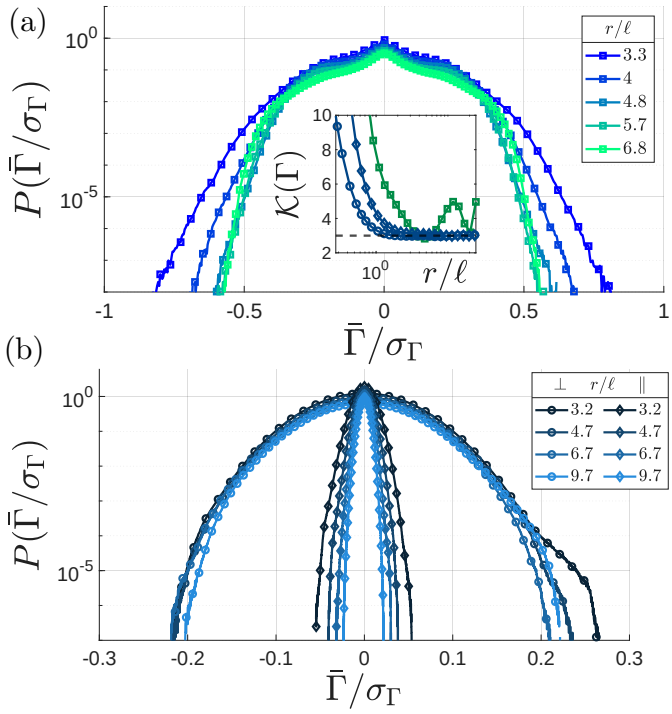

FIG. 3: PDFs of the velocity circulation for different loop sizes $r/\ell > 1$, scaled by the standard deviation σ_Γ. (a) shows the Taylor-Green simulation, while *(b)* shows both of the normal fluid parallel (diamonds) and perpendicular (circles) components. The inset of (a) shows the flatness $\mathcal{K}(\Gamma) = \langle|\Gamma|^4\rangle/\sigma_\Gamma^4$, with the same color scheme as in Fig. 2. The black dashed line marks the Gaussian flatness of $\mathcal{K} = 3$. See the Supplementary materials for the SF PDFs.

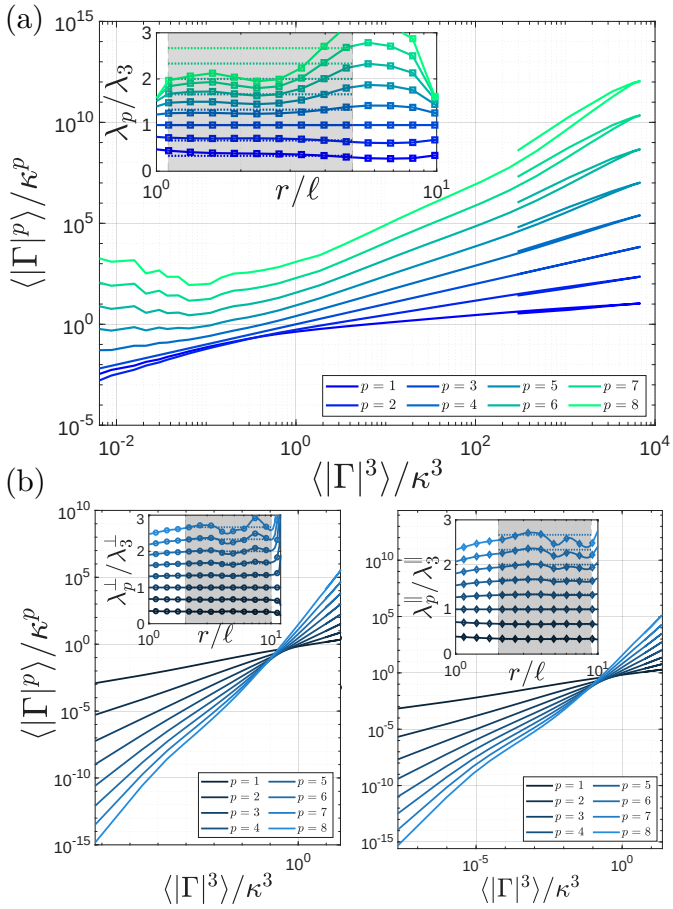

FIG. 4: Circulation moments $\langle|\Gamma|^p\rangle$ in extended self-similarity (ESS) using $p = 3$. (a) shows the Taylor-Green simulation, while the left and right panels of (b) are the normal fluid perpendicular and parallel component respectively. The insets of each plot give the local slope, where $\lambda_p/\lambda_3 = \mathrm{d}\left[\log\langle|\Gamma|^p\rangle\right]/\mathrm{d}\left[\log\langle|\Gamma|^3\rangle\right]$ and the horizontal lines correspond to the K41 scalings $\lambda_p^{K41} = 4p/3$. The shaded regions indicate the classical region where the data used to estimate the exponents.

ing of $\langle|\Gamma|^2|\rangle \sim r^4$ for small loop sizes r , as a result of smoothness at very small scales [5].

The cross-over from the quantum $r \ll \ell$ to the classical $r \gtrsim \ell$ marks a stark contrast in the superfluid circulation variance scaling. While the TG scales in accordance with a partial polarization of vortices where $r^{8/3}$ [6], the CF scaling, appears to follow a scaling of $\sim r^{1.58}$, a weaker scaling than for a fully random tangle of vortex lines which exhibits r^2 scaling in the classical range. Remarkably both components of the SF and NF statistics of CF appear to adhere to this scaling law for loops $r \gtrsim \ell$. For the remainder of this paper, we will only focus on the classical range where the loop sizes $r > \ell$.

In fully-developed isotropic classical turbulence, velocity circulation statistics adhere to a strictly non-Gaussian distribution with long tails [7]. Deviations from Gaussian statistics are the hallmark of intermittency, and represent a deviation from self-similar scaling which are evident in the TG simulations shown in Fig. 3a. The circulation PDF of the NF components differs very strongly (see Fig. 3b). Strikingly, we see a complete collapse to Gaussian statistics for the perpendicular components, while the parallel component exhibits very small deviations. We show this collapse by computing the flatness $\mathcal{K}(\Gamma) = \langle|\Gamma|^4\rangle/\sigma_\Gamma^4$, where σ_Γ is the standard deviation $\sqrt{\langle|\Gamma|^2\rangle}$. The flatness is displayed in the inset of Fig. 3a. In the classical regime the NF components monotonically decay to the Gaussian value of $\mathcal{K} = 3$, while the non-Gaussian TG simulation deviates in the same region. Indeed we observe that the presence of quantized vortices suppresses the intermittent behaviour of the classically-driven NF.

As is customary in the classical turbulence, we will characterize the intermittency by measuring the deviation of the circulation moments of order p given by $\langle|\Gamma|^p\rangle$ from the self-similar K41 scaling. The TG and NF moments are shown in Fig. 4, where we have plotted the circulation moments in extended self-similarity (ESS) using

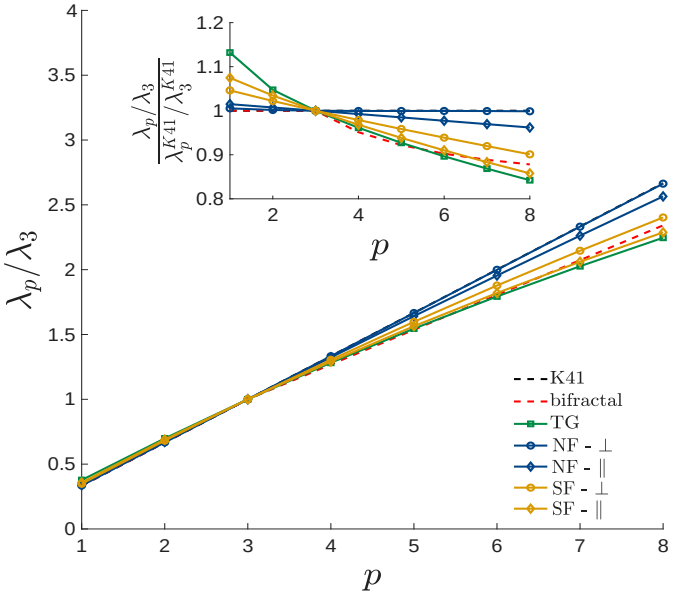

FIG. 5: Scaling exponents of velocity circulation moments, estimated within the classical range $r > \ell$. The colour scheme and linestyles is the same as in Fig. 2. The black dashed line represents the self-similar K41 scaling $\lambda_p^{K41} = 4p/3$. The inset shows the proportional deviation from K41 theory.

the third-order circulation moment $\langle|\Gamma|^3\rangle$. In this way, we define the scaling exponents λ_p as

$$\langle|\Gamma|^p\rangle \sim \left[\langle|\Gamma|^3\rangle\right]^{(\lambda_p/\lambda_3)p} \tag{3}$$

In order to compute the scaling exponents, we find the local slope of the moments in ESS, which is given by

$$\left(\frac{\lambda_p}{\lambda_3}\right)(r) = \frac{\mathrm{d}\left[\log\langle|\Gamma|^p\rangle\right]}{\mathrm{d}\left[\log\langle|\Gamma|^3\rangle\right]} \tag{4}$$

As the local-slope of pure power-law functions is flat, we look for flat regions where the loop sizes are $r > \ell$, and then average over the selected regions.

[1] L. Galantucci, A. W. Baggaley, C. F. Barenghi, and G. Krstulovic, A new self-consistent approach of quantum turbulence in superfluid helium, Eur. Phys. J. Plus **135**, 547 (2020).

[2] KW. Schwarz, Three-dimensional vortex dynamics in superfluid 4He, Phys. Rev. B **38**, 2398 (1988).

[3] A. W. Baggaley and C. F. Barenghi, Tree Method for Quantum Vortex Dynamics, J. Low Temp. Phys. **166**, 3 (2012).

[4] N. P. Müller, J. I. Polanco, and G. Krstulovic, Intermittency of Velocity Circulation in Quantum Turbulence, Phys. Rev. X **11**, 011053 (2021).

[5] K. P. Iyer, K. R. Sreenivasan, and P. K. Yeung, Circulation in High Reynolds Number Isotropic Turbulence is a Bifractal, Phys. Rev. X **9**, 041006 (2019).

[6] V. S. L'vov, S. V. Nazarenko, and O. Rudenko, Bottleneck crossover between classical and quantum superfluid turbulence, Phys. Rev. B **76**, 024520 (2007).

[7] M. Wilczek and R. Friedrich, Dynamical origins for non-Gaussian vorticity distributions in turbulent flows, Phys. Rev. E **80**, 016316 (2009).